Cellulose/Syndiotactic Polypropylene Composites: Effects of Maleated Polypropylene as a Compatibilizer and Silanized Cellulose on the Morphology and Tensile Properties

Hisayuki Nakatani,[1] Kazuya Hashimoto,[1] Kensuke Miyazaki,[1] Minoru Terano[2]

[1]*Department of Biotechnology and Environmental Chemistry, Kitami Institute of Technology, 165 Koen-Cho, Kitami, Hokkaido 090-8507, Japan*
[2]*School of Materials Science, Japan Advanced Institute of Science and Technology, 1-1 Asahidai, Nomi, Ishikawa 923-1292, Japan*

Received 13 November 2008; accepted 18 February 2009
DOI 10.1002/app.30298
Published online 17 April 2009 in Wiley InterScience (www.interscience.wiley.com).

ABSTRACT: To improve the interaction between syndiotactic polypropylene (SPP) and fibrous cellulose (FC), the effects of the addition of maleated polypropylene (MAPP) and FC surface modification with 3-aminopropyltriethoxysilane (APTES) on SPP/FC composites were studied with respect to the morphology and the tensile properties. The addition of MAPP brought about an improvement in the interfacial adhesion between SPP and FC according to scanning electron microscopy observations and tensile testing. This improvement was, however, less effective than the improvement in the interfacial adhesion between isotactic polypropylene (IPP) and FC. SPP and MAPP partially or microscopically phase-separated because of the IPP-like polymer chain structure of MAPP. With respect to the compatibility between SPP and FC, FC surface modification with APTES was more suitable. The increase in Young's modulus was remarkable in the SPP/silanized FC composite with APTES. The tensile strength of the SPP/silanized FC composite with APTES was, however, considerably lower than that of the SPP/FC/MAPP composite. These results suggest that interfacial improvement between SPP and FC requires a compatibilizer or a surface modifier with a suitable primary structure. © 2009 Wiley Periodicals, Inc. J Appl Polym Sci 113: 2022–2029, 2009

Key words: compatibility; composites; morphology; poly(propylene) (PP)

INTRODUCTION

Cellulose has been used for the manufacture of paper for a long time. Cellulose is low-cost, has a high modulus, and is renewable and biodegradable. Recently, cellulose has attracted much attention as a composite material[1–10] because it has great potential for the preparation of composite materials with high modulus and renewability. As the most popular composite based on cellulose, the composite with isotactic polypropylene (IPP) has been extensively prepared. This is due to the commercial importance of IPP in industrial products. In the case of the composite, fibrous cellulose (FC) has generally been used as the cellulose source because it has been expected instead of glass or carbon fibers.

There is another type of crystalline polypropylene (PP) polymer: syndiotactic polypropylene (SPP).[11,12] SPP has excellent properties with respect to resistance against thermooxidative degradation,[13–15] and its composites containing glass fillers and nanosilicates have recently attracted considerable interest for their reinforced tensile properties.[16,17] In SPP composites, the compatibilizer and the surface modifier strongly affect the morphology and crystallization of the SPP matrix. They are key points for the reinforcement of the tensile properties. An SPP composite containing FC (SPP/FC) will also be expected to show reinforcement of the tensile properties. In addition, an SPP/FC composite is expected to have other attractive properties, such as renewability and biodegradability. However, there have been no studies on SPP/FC composites.

In this study, an SPP/FC composite was extensively studied to clarify the effects of maleated polypropylene (MAPP) as a compatibilizer and silanized FC with 3-aminopropyltriethoxysilane (APTES) on the morphology and the tensile properties

EXPERIMENTAL

Materials

SPP (trade name Total 1751) was supplied by Sanwayuka Industry Co. (Kariya, Japan). The number-

Correspondence to: H. Nakatani (nakatani@chem.kitami-it.ac.jp).

average molecular weight (M_n) and polydispersity (M_w/M_n, where M_w is the weight-average molecular weight) were 3.5×10^4 and 3.0, respectively. IPP was purchased from Sigma–Aldrich (St. Louis, MO). M_n and M_w/M_n were 5.0×10^4 and 3.8, respectively. FC (W-100GK) was donated by Nippon Paper Chemicals Co., Ltd. (Tokyo, Japan). FC was dried in a desiccator for 7 days before preparation. The moisture of FC was below 0.7 wt %. The dimensions of FC were over 90% past a 100-mesh screen, and the average length was about 37 μm. MAPP was purchased from Sigma–Aldrich. The maleic anhydride content was about 8 wt %. M_n and M_w/M_n were 3.9×10^3 and 2.3, respectively. APTES and ethanol were purchased from Shinetsu Silicon Chemicals Co. (Tokyo, Japan) and Wako Pure Chemical Industry (Osaka, Japan), respectively. These were used without further purification.

Preparation of silanized FC

The mixing of a 30-mL ethanol solution of APTES and FC (1 g) was performed with a 0.1-L glass equipped with a stirrer at 23°C for 24 h. The mixing ratios of APTES to FC were 1, 2, 3, 4, and 5 wt %. The solvent ethanol was evaporated with a rotary evaporator. The FC that was obtained was dried at 60°C for 6 h in a vacuum oven and was used as silanized FC.

Preparation of the composites

The composites were prepared with an Imoto Seisakusyo (Kyoto, Japan) IMC-1884 melting mixer. All mixtures were prepared for each weight ratio. After a small amount (ca. 0.5%) of a phenolic antioxidant (AO-60, Adekastab, Tokyo, Japan) was added, the mixing was performed at 190°C at 60 rpm for 5 min. The obtained composites were molded into films (100 μm) by compression molding at 190°C under 40 MPa for 5 min.

Wide-angle X-ray diffraction (WAXD) measurements

WAXD diffractograms were recorded in reflection geometry at 2° (2θ/min) under Ni-filtered Cu Kα radiation with a Rigaku (Tokyo, Japan) XG-Rint 1200 diffractometer.

Scanning electron microscopy (SEM) and SEM/electron dispersive spectrometry (EDS) analyses

SEM and SEM/EDS analyses were carried out with a JEOL (Tokyo, Japan) JSM-5800 at 20 kV. The plate of a sample was fractured in liquid nitrogen, and then the fractured surface was cut with a microtome to obtain a flat surface. The obtained sample was oxidatively degraded in an oven at 100°C and then was sputter-coated with gold. Carbon, oxygen, and silicon contents were measured with an EDS apparatus (INCA Microanalysis, Oxford Instruments, Abingdon, UK).

Tensile testing

Stress–strain behavior was observed with a Shimadzu (Tokyo, Japan) EZ-S at a crosshead speed of 3 mm/min. The sample specimens were cut ($30 \times 2 \times 0.1$ mm^3), and the gauge length was 10 mm. All tensile testing was performed at 20°C. The values of Young's modulus were obtained from the slopes of the stress–strain curves (until about 1% of the strain value). All results were the average values of 10 measurements.

Differential scanning calorimetry (DSC) measurements

DSC measurements were made with a Shimadzu DSC-60. Samples of about 5 mg were sealed in aluminum pans. The measurement of the samples was carried out at a heating rate of 10°C/min under a nitrogen atmosphere.

RESULTS AND DISCUSSION

WAXD patterns of FC, SPP, and an SPP (70%)/FC (30%) composite are shown in Figure 1. The crystal forms of FC and SPP are cellulose I (native form)[18] and form I (orthorhombic),[19,20] respectively. The WAXD pattern of the composite shows the overlapping pattern of the FC and SPP crystal forms,

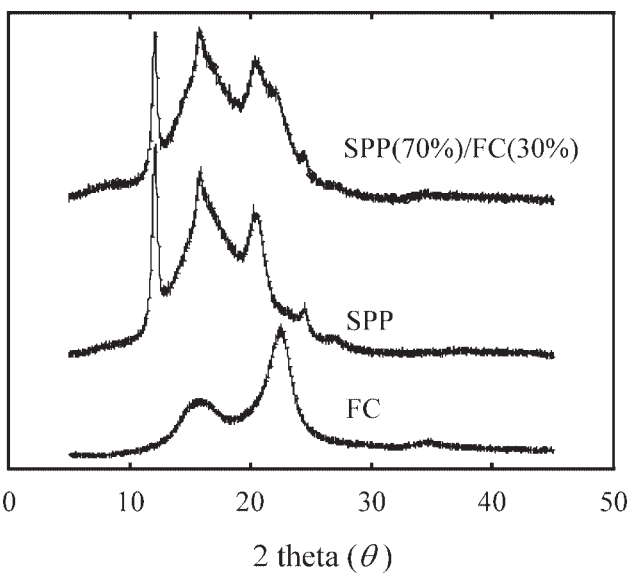

Figure 1 WAXD patterns of FC, SPP, and the SPP/cellulose composite.

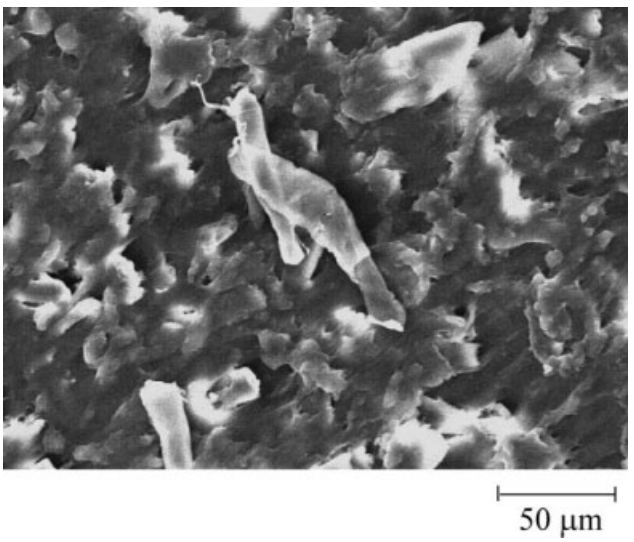

Figure 2 SEM micrograph of the SPP (70%)/FC (30%) composite.

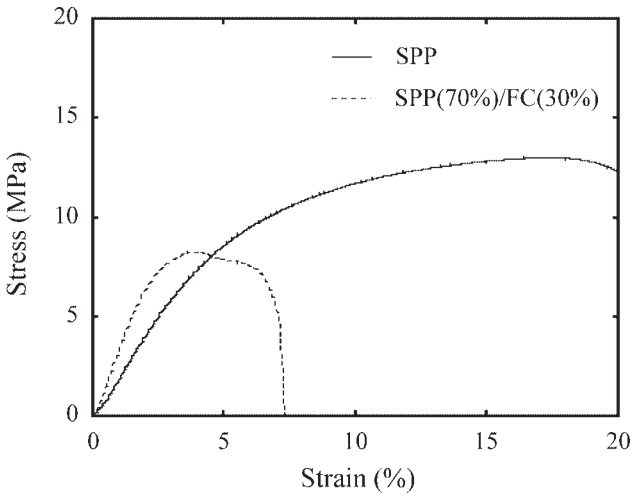

Figure 3 Stress–strain curves of SPP and the SPP (70%)/FC (30%) composite.

suggesting that the existence of FC has no effect on the crystal form of the SPP matrix.

An SEM micrograph of the fractured surface of SPP (70%)/FC (30%) is shown in Figure 2. The micrograph shows that there are many FC aggregates. In addition, the FC surfaces seem to be quite smooth, and the FCs are not fractured. Figure 3 shows the stress–strain curves of SPP and SPP (70%)/FC (30%). Although the composite exhibits a higher tensile Young's modulus than SPP, the values of the tensile strength and elongation at break are considerably lower than those of SPP. These results suggest that the interfacial adhesion between FC and SPP is poor and requires improvement.

The stress–strain curves of SPP (70%)/FC (30%) with the addition of MAPP as a compatibilizer are shown in Figure 4, and the data for the tensile properties are summarized in Table I. MAPP as a compatibilizer certainly brings about an improvement in the interface between FC and SPP. In particular,

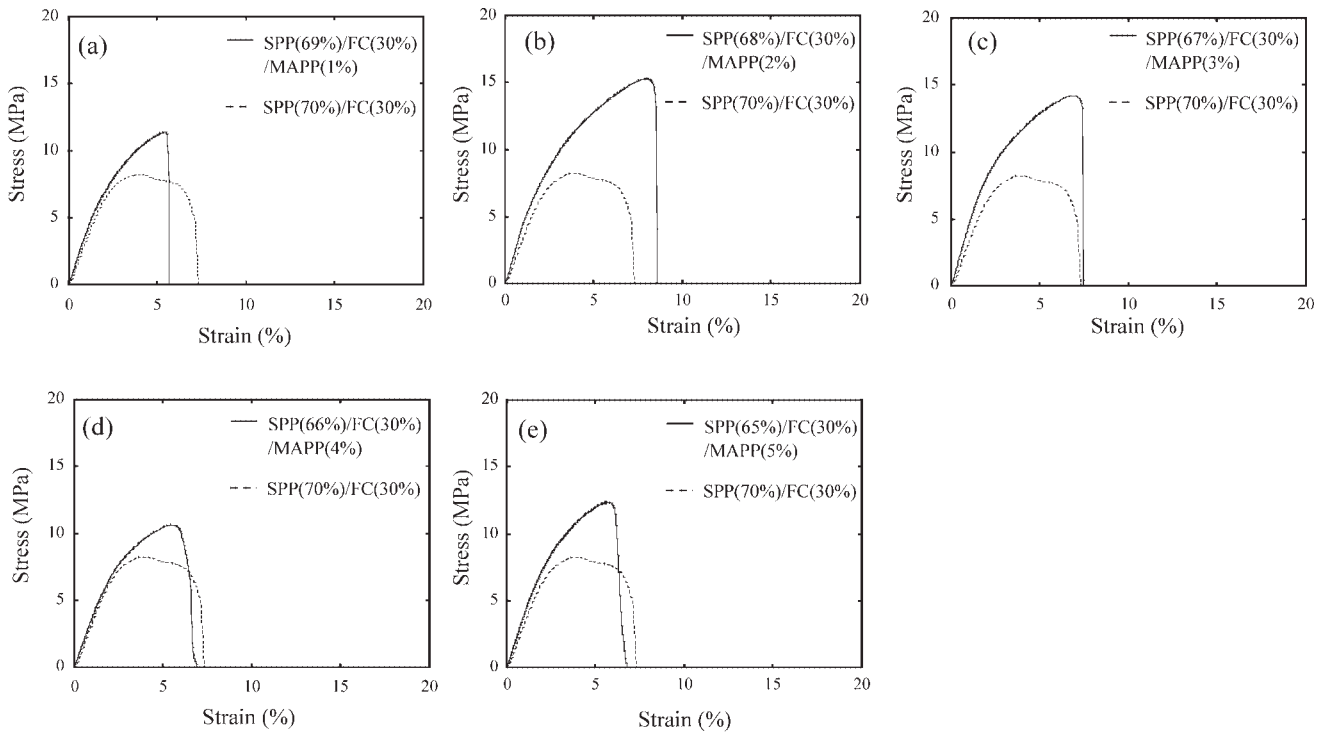

Figure 4 Stress–strain curves of the SPP/FC/MAPP and SPP/FC composites.

TABLE I
Tensile Properties of the SPP/FC/MAPP Composites with Various MAPP Contents

Sample	Young's modulus (MPa)	Tensile strength (MPa)	Elongation at break (%)
SPP (70%)/FC (30%)	386 ± 27	8.5 ± 0.2	7.3 ± 0.2
SPP (69%)/FC (30%)/ MAPP (1%)	393 ± 11	11.1 ± 0.3	5.8 ± 0.1
SPP (68%)/FC (30%)/ MAPP (2%)	436 ± 52	14.9 ± 0.6	8.8 ± 0.2
SPP (67%)/FC (30%)/ MAPP (3%)	475 ± 16	13.9 ± 0.3	7.6 ± 0.1
SPP (66%)/FC (30%)/ MAPP (4%)	360 ± 41	10.8 ± 0.3	7.0 ± 0.2
SPP (65%)/FC (30%)/ MAPP (5%)	372 ± 27	12.2 ± 0.4	6.5 ± 0.2

with MAPP concentrations of 2 and 3%, the improvement in the tensile properties is considerably higher. These values of Young's modulus and the tensile strength are about 20 and 70% higher than those of SPP (70%)/FC (30%), respectively. An SEM micrograph of the fractured surface of SPP (69%)/FC (30%)/MAPP (1%) is shown in Figure 5. Many rodlike FCs are partially attached to the SPP matrix. The SEM micrograph reveals that the addition of MAPP causes an improvement in the interface between FC and SPP.

However, in the case of SPP/FC, the improvement with the MAPP compatibilizer in the interface is lower in comparison with the IPP/FC composite. The stress–strain curves of IPP (70%)/FC (30%) and IPP (68%)/FC (30%)/MAPP (2%) are shown in Figure 6. The tensile properties of IPP/FC/MAPP with

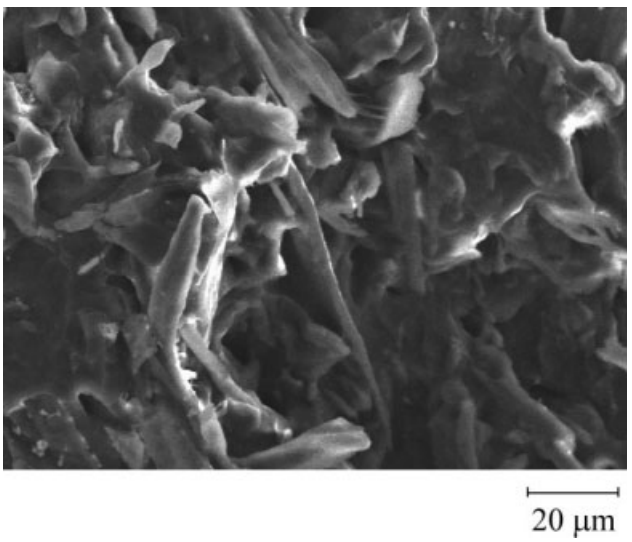

Figure 5 SEM micrograph of the SPP (69%)/FC (30%)/ MAPP (1%) composite.

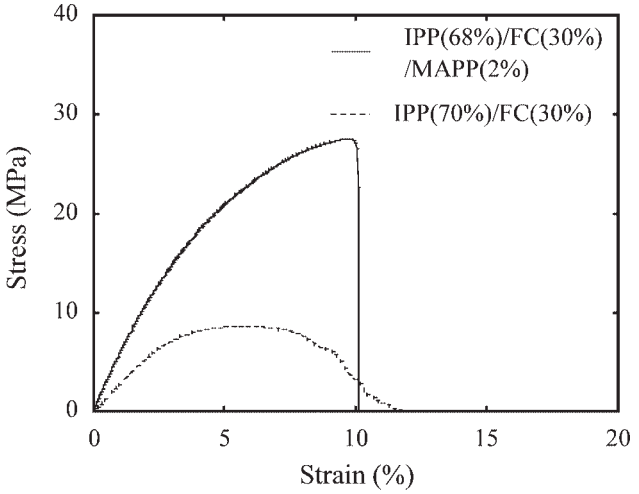

Figure 6 Stress–strain curves of the IPP/FC/MAPP and IPP/FC composites.

various MAPP contents are summarized in Table II. All the IPP/FC/MAPP composites show marked improvements in the tensile strength and Young's modulus in comparison with IPP/FC. In particular, with a 2% concentration of MAPP, the values of Young's modulus and the tensile strength are about 200 and 300% higher than those of IPP (70%)/FC (30%), respectively. MAPP as a compatibilizer brings about improvements in the interface between FC and IPP more effectively in comparison with SPP/FC. As shown in Figure 7, FC is buried in the IPP matrix, and the interface is blurred. This micrograph demonstrates that FC and IPP are bound tightly by the compatibilizer MAPP.

Esterification between OH groups in FC and maleic anhydride groups in MAPP occurs.[21–23] The grafted FC leads to reinforcement of the interface in both SPP/FC and IPP/FC. The main-chain structure of MAPP is, however, isotactic (i.e., IPP). According to Mülhaupt and coworkers,[16,24] blends of IPP and

TABLE II
Tensile Properties of the IPP/FC/MAPP Composites with Various MAPP Contents

Sample	Young's modulus (MPa)	Tensile strength (MPa)	Elongation at break (%)
IPP (70%)/FC (30%)	336 ± 72	8.7 ± 0.2	12.0 ± 0.1
IPP (69%)/FC (30%)/ MAPP (1%)	527 ± 46	12.9 ± 0.2	7.2 ± 0.4
IPP (68%)/FC (30%)/ MAPP (2%)	671 ± 73	27.3 ± 0.4	10.3 ± 0.2
IPP (67%)/FC (30%)/ MAPP (3%)	630 ± 30	22.4 ± 0.7	7.4 ± 0.6
IPP (66%)/FC (30%)/ MAPP (4%)	552 ± 12	19.6 ± 0.9	7.5 ± 0.1
IPP (65%)/FC (30%)/ MAPP (5%)	466 ± 89	14.1 ± 0.4	5.6 ± 0.4

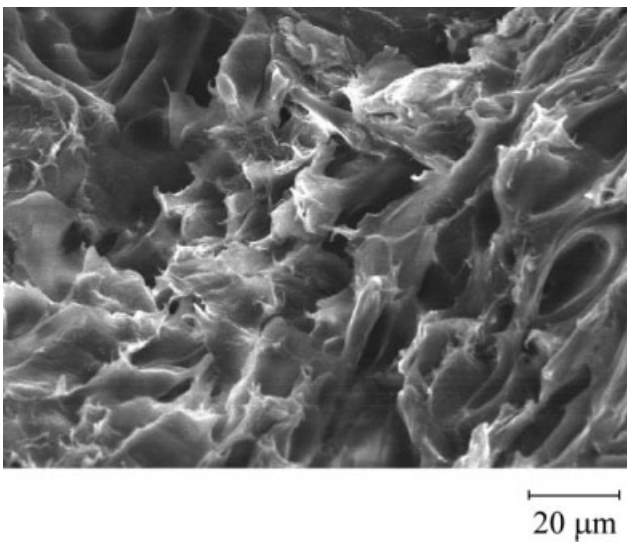

Figure 7 SEM micrograph of the IPP (65%)/FC (30%)/MAPP (5%) composite.

SPP are immiscible. In the case of SPP/FC, the improvement effect of the compatibilizer MAPP on the tensile properties and interface is considerably inferior to that for IPP/FC. This behavior is due to the phase separation between SPP and MAPP. SEM micrographs of fractured surfaces of SPP (70%)/MAPP (30%) and IPP (70%)/MAPP (30%) blends are shown in Figure 8. Both surfaces are rugged because of the spherulite structures of SPP, MAPP, and IPP. Although the irregularity of the SPP (70%)/MAPP (30%) surface is lower [in other words, the spherulite size is smaller than that of IPP (70%)/MAPP (30%)], the surface morphology is similar to that of IPP (70%)/MAPP (30%), suggesting that there is no macrophase-separation structure in SPP (70%)/MAPP (30%). The melting behavior of the SPP crystalline part is affected by the existence of MAPP, as shown in Figure 9. The single peak of the melting temperature (T_m) becomes multiple, and the new multiple peaks, which are assigned to the MAPP part, appear around 160°C. However, as shown in Figure 10, the T_m peak of IPP/FC is unchanged by the existence of MAPP, and this indicates that IPP and MAPP have

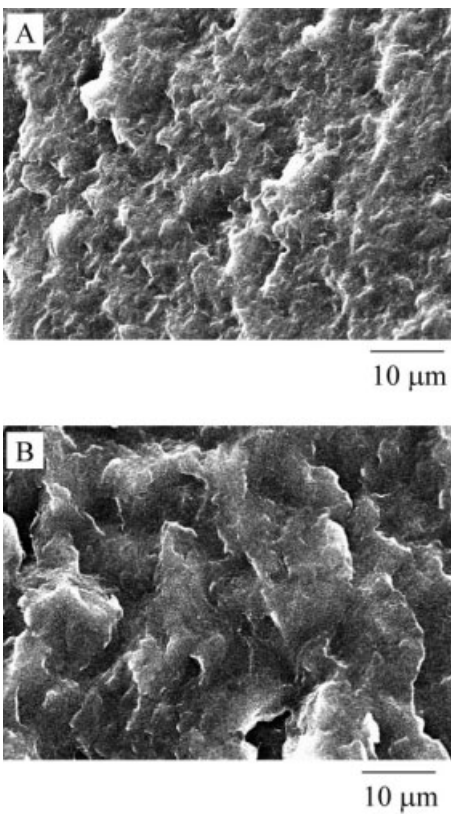

Figure 8 SEM micrographs of the (A) SPP (70%)/MAPP (30%) and (B) IPP (70%)/MAPP (30%) composites.

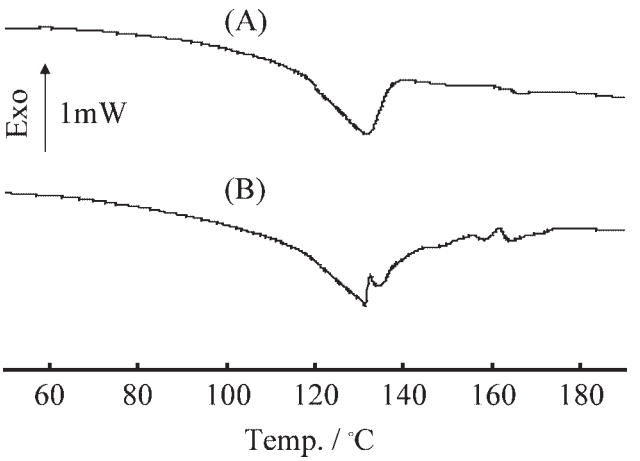

Figure 9 DSC curves of the (A) SPP (70%)/FC (30%) and (B) SPP (65%)/FC (30%)/MAPP (5%) composites.

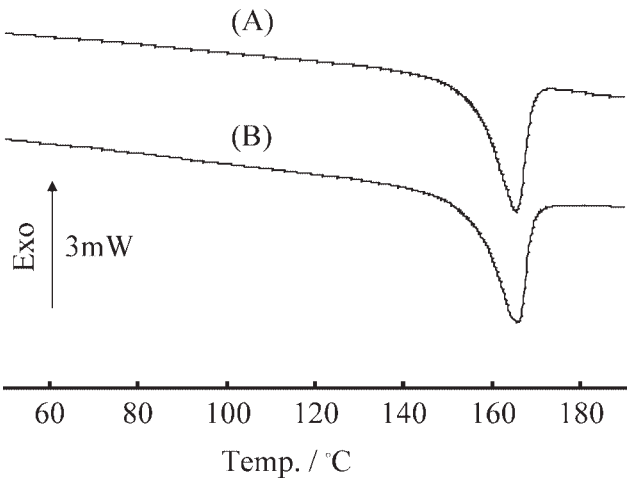

Figure 10 DSC curves of the (A) IPP (70%)/FC (30%) and (B) IPP (65%)/FC (30%)/MAPP (5%) composites.

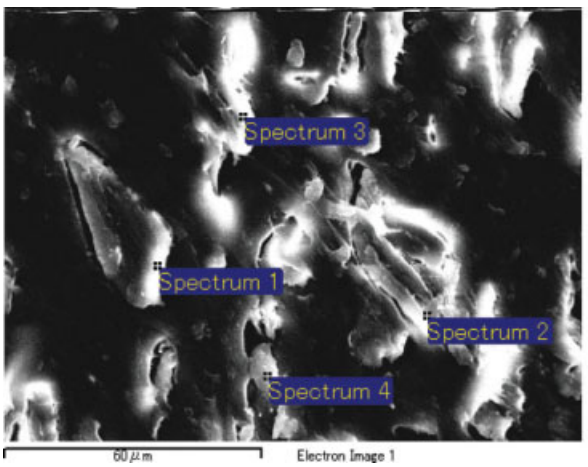

Spot (Spectrum)	C [%]	O [%]	Si [%]
1	74.18	25.65	0.17
2	76.03	23.92	0.04
3	83.79	15.10	1.11
4	77.19	22.64	0.17

Atomic percent.

Figure 11 SEM microphotograph of the surface of the SPP (70%)/silanized FC (30%) composite with 5% APTES and sampling spot compositions measured by EDS analysis. [Color figure can be viewed in the online issue, which is available at www.interscience.wiley.com.]

the same crystal form (monoclinic). It seems from this melting behavior that SPP and MAPP partially or microscopically take a phase-separation structure.[16] In addition, in the cases of higher MAPP contents such as 4 and 5%, the SPP/FC/MAPP composites show lower Young's moduli than the SPP/FC composite (see Table I). This behavior is due to the increase in the phase-separation structure. In fact, in the case of the IPP/FC/MAPP composites with 4 or 5% MAPP, although the values of the tensile strength and Young's modulus decrease in comparison with those of the composite containing the optimum MAPP concentration of 2%, the composites exhibit much better values than those of the IPP/FC composites (see Table II). To acquire superior tensile properties in SPP/FC, another compatibilizer is required.

Karnani et al.[25] reported that there was a significant improvement in the mechanical properties of a PP/kenaf fiber composite through the surface modification of kenaf with an alkylaminotrialkoxysilane compound. It seems that the silane compound could be applied to SPP. The application of the silane compound would be more suitable for improvements in the interface between FC and SPP. Figure 11 shows an SEM microphotograph of the surface of the SPP (70%)/silanized FC (30%) composite with 5% APTES and sampling spot compositions measured by EDS analysis. Si atoms can be detected at all sampling spots, and partial adhesion between FC and SPP can be observed. These results indicate that FC is extensively covered with APTES, which acts as a compatibilizer of SPP/FC. Interestingly, the silanized FC disperses finely in the SPP matrix in comparison with SPP/FC/MAPP. However, in SPP/FC/MAPP, FC is aggregated in the SPP matrix (see Fig. 5). The dispersion behavior of the silanized FC is similar to that of a modified FC with a surfactant.[26]

Figure 12 shows DSC curves of SPP (70%)/silanized FC (30%) with 2% APTES and SPP (70%)/silanized FC (30%) with 5% APTES. In both samples of SPP/silanized FC with APTES, T_m is the same (ca. 130°C), and its peak shape is unchanged. The DSC curves indicate that the SPP crystalline part is unaffected by the silanized FC.

Figure 13 shows the stress–strain curves of SPP/silanized FC composites with APTES and SPP/FC composites, and the obtained tensile properties are summarized in Table III. The increases in Young's modulus are remarkable in SPP/silanized FC with APTES. The values of SPP/FC with APTES range from about 500 to 540 MPa, and they are

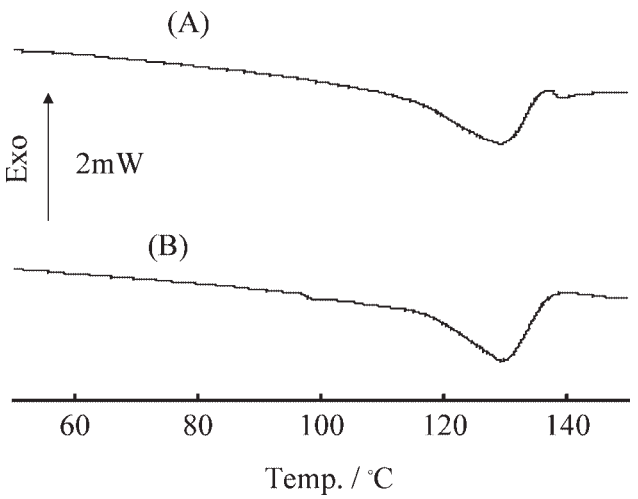

Figure 12 DSC curves of (A) the SPP (70%)/silanized FC (30%) composite with 2% APTES and (B) the SPP (70%)/silanized FC (30%) composite with 5% APTES.

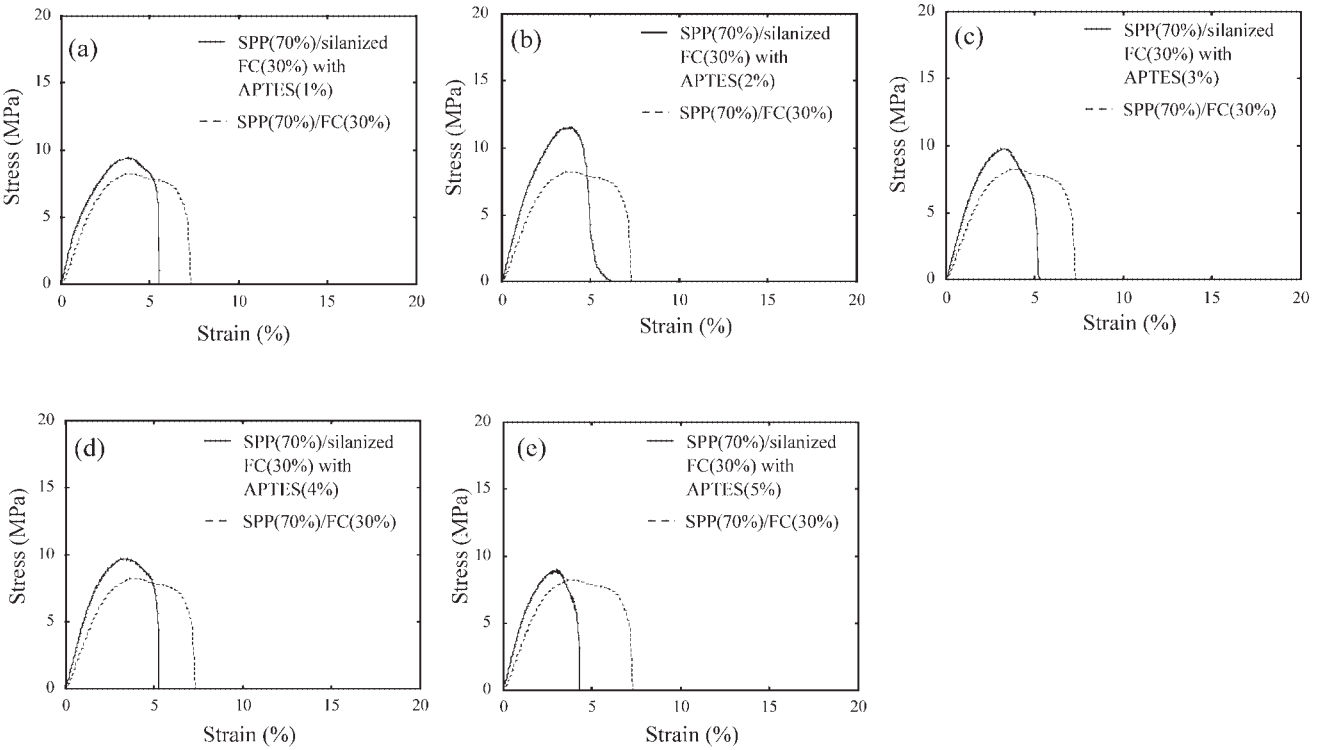

Figure 13 Stress–strain curves of the SPP/silanized FC and SPP/FC composites.

considerably higher than those of SPP/FC and SPP/FC/MAPP, as shown in Figure 14. In contrast, the values of the tensile strength of SPP/silanized FC with APTES are considerably lower than those of SPP/FC/MAPP and close to those of SPP/FC (see Fig. 15). Although the compatibility of SPP and silanized FC is good, the strength of the interface is poor.

CONCLUSIONS

With the aim of improving compatibility between SPP and FC, the effects of the addition of MAPP and FC surface modification with a silane compound on SPP/FC composites were studied with respect to the morphology and tensile properties. The addition of MAPP brought about an improvement in the interfacial adhesion between SPP and FC according to SEM observations and tensile testing. The improvement was, however, less effective than the improvement in the interfacial adhesion between IPP and FC. SPP and MAPP partially or microscopically took a phase-separation structure because the polymer chain structure of MAPP was IPP. This phase-separation structure was responsible for the lower additive effect of MAPP. From the viewpoint of compatibility between SPP and FC, FC surface modification with APTES was more suitable. The increase in Young's modulus was remarkable in SPP/silanized FC with APTES. The tensile strength of SPP/silanized FC with APTES was, however, considerably lower than that of SPP/FC/MAPP. Although the compatibility

TABLE III
Tensile Properties of the SPP (70%)/Silanized FC (30%) Composites with Various APTES Contents

Sample: SPP (70%)/FC (30%) with APTES	Young's modulus (MPa)	Tensile strength (MPa)	Elongation at break (%)
0%	386 ± 27	8.5 ± 0.2	7.3 ± 0.2
1%	515 ± 70	9.2 ± 0.9	6.1 ± 0.8
2%	529 ± 14	11.4 ± 0.7	6.5 ± 0.3
3%	497 ± 60	9.4 ± 0.5	5.1 ± 0.3
4%	494 ± 21	9.4 ± 0.3	5.4 ± 0.1
5%	537 ± 73	9.0 ± 0.4	4.5 ± 0.1

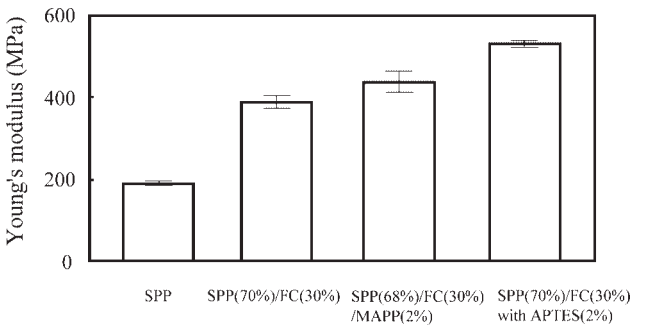

Figure 14 Comparison of the Young's moduli of SPP, SPP/FC, SPP/FC/MAPP, and SPP/FC with APTES.

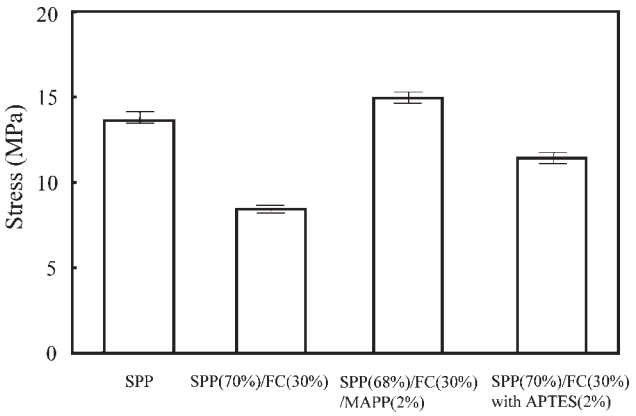

Figure 15 Comparison of the tensile strengths of SPP, SPP/FC, SPP/FC/MAPP, and SPP/FC with APTES.

of SPP and silanized FC was good, the strength of the interface was poor.

In conclusion, these results suggest that interfacial improvement between SPP and FC requires a compatibilizer or a surface modifier with excellent compatibility.

References

1. Takase, S.; Shiraishi, N. J Appl Polym Sci 1989, 37, 645.
2. Maldas, D.; Kokta, B. V.; Daneault, C. J Appl Polym Sci 1989, 37, 751.
3. Raj, R. G.; Kokta, B. V.; Maldas, D.; Daneault, C. J Appl Polym Sci 1989, 37, 1089.
4. Hedenberg, P.; Gatenholm, P. J Appl Polym Sci 1996, 60, 2377.
5. Zhang, F.; Qiu, W.; Yang, L.; Endo T. J Mater Chem 2002, 12, 24.
6. Qiu, W.; Zhang, F.; Endo, T.; Hirotsu, T. J Appl Polym Sci 2003, 87, 337.
7. Qiu, W.; Zhang, F.; Endo, T.; Hirotsu, T. J Appl Polym Sci 2004, 91, 1703.
8. Felix, J. M.; Gatenholm, P. J Appl Polym Sci 1991, 42, 609.
9. Qiu, W.; Zhang, F.; Endo, T.; Hirotsu, T. J Appl Polym Sci 2004, 94, 1326.
10. Hristov, V. N.; Vasileva, S. T.; Krumova, M.; Lach, R.; Michler G. H. Polym Compos 2004, 25, 521.
11. Natta, G.; Pasquon, P.; Zambelli, A. J Am Chem Soc 1962, 84, 6255.
12. Ewen, J. A.; Jones, R.; Razavi, A.; Ferrara J. D. J Am Chem Soc 1988, 110, 6255.
13. Mori, H.; Hatanaka, T.; Terano, M. Macromol Rapid Commun 1997, 18, 157.
14. Hatanaka, T.; Mori, H. T.; Terano, M. Polym Degrad Stab 1999, 65, 271.
15. Nakatani, H.; Suzuki, S.; Tanaka, T.; Terano, M. Polymer 2005, 46, 12366.
16. Kaempfer, D.; Thomann, R.; Mülhaupt, R. Polymer 2002, 43, 2909.
17. Stricker, F.; Bruch, M.; Mülhaupt, R. Polymer 1997, 38, 5347.
18. Borysiak, S.; Garbarczyk, J. Fibers Text Eastern Eur 2003, 11, 104.
19. Guadagno, L.; Naddeo, C.; Vittoria, V.; Meille, S. V. Macromolecules 2005, 38, 8755.
20. Ma, W.; Yu, J.; He, J.; Wang, D. Polymer 2007, 48, 1741.
21. Felix, J. M.; Gatenholm, P. J Appl Polym Sci 1991, 42, 609.
22. Miyazaki, K.; Okazaki, N.; Terano, M.; Nakatani, H. J Polym Environ 2008, 16, 267.
23. Miyazaki, K.; Moriya, K.; Okazaki, N.; Terano, M.; Nakatani, H. J Appl Polym Sci 2009, 111, 1835.
24. Thomann, R.; Kressler, J.; Setz, S.; Wang, C.; Mülhaupt, R. Polymer 1996, 1, 774.
25. Karnani, R.; Krishnan, M.; Narayan R. Polym Eng Sci 1997, 37, 476.
26. Ljungberg, N.; Bonini, C.; Bortolussi, F.; Boisson, C.; Heux, L.; Cavaillé, J. Y. Biomacromolecules 2005, 6, 2732.